Local layer-by-layer growth of Ni on hydrogen-terminated diamond C(111): A combined helium-atom scattering and XPS study

J. Braun and J. P. Toennies
Max-Planck-Institut für Strömungsforschung, Bunsenstraße 10, D-37073 Göttingen, Germany

Ch. Wöll
Physikalische Chemie I, Universität Bochum, D-44780 Bochum, Germany
(Received 17 March 1999)

The growth, structure, and phonon dynamics of Ni islands deposited on H(1×1)C(111) was studied using high-resolution helium atom scattering and x-ray photoelectron spectroscopy. Depending on the amount of deposited nickel the islands formed at temperatures of 800 K are between 6- and 20-monolayers (ML) high and cover 50 to 85 % of the surface. Since the height distribution of these islands is very narrow a layer-resolved study of the phonon dynamics of these islands has been possible. For islands with a thickness of 6 ML an energy gap of 3 meV is observed at the center of the surface Brillouin zone corresponding to a vertical vibration of the whole Ni island with respect to the substrate. A lattice-dynamical analysis based on a rigid-substrate approximation indicates that force constant coupling of the Ni atoms to the surface amounts to only 15.75 N/m, suggesting only a weak metal-substrate interaction. [S0163-1829(99)02839-8]

I. INTRODUCTION

In recent years, the growth of metal films on solid substrates that are wetted by the metal has been extensively studied.[1] Quite frequently a layer-by-layer growth mode is observed and this has stimulated a large number of studies on thin two-dimensional (2D) metal layers on metal substrates.[2] One complication in understanding these systems arises from the electronic coupling between the deposited 2D metal film and the metallic substrate. To avoid such a coupling there have been several attempts to grow metal films on insulating substrates,[3] however, here it is usually difficult to find systems that wet each other. For nonwetting substrates a completely different growth scenario is often found and generally a three-dimensional (3D) or Volmer-Weber growth is expected.[4] Special kinetic limitations can give rise to a quasi-layer-by-layer growth.[3] A particular interesting system is the growth of metal films on metal oxides, e.g., Cu on ZnO surfaces,[5] where complex growth modes have been observed.

In the present investigation Ni films have been grown on diamond substrates with the aim to produce thin highly ordered metal layers on a large band-gap insulator. To rule out any coupling effects the insulator with the largest band gap (5.47 eV) available, diamond, has been chosen as the substrate. Moreover, in order to suppress the possibility of unwanted chemical interaction between metal and substrate the diamond surface has been passivated by hydrogen[6] before metal deposition. As will be demonstrated below, this strategy was successful and led to the growth on the diamond substrate of highly structurally ordered finite-size epitaxial Ni-layers, which are only slightly coupled to the substrate by weak dispersion forces.

Several experiments on the adsorption of metals on diamond have been reported in the past. However, the majority of the previous studies has focused on electronic properties of the interface such as conductance and contact characteristics[7,8] rather than on structural or dynamical properties. So far only few experiments on the growth and structure of adsorbed metals have been carried out at low coverages where the influence of the interface is expected to dominate. For the Ni-H(1×1)C(111) diamond system, which has a small lattice mismatch of only 1.4%, Lurie and Wilson[9] found epitaxial growth of Ni at a surface temperature around 800 K using low-energy electron diffraction (LEED) and Auger electron spectroscopy. This result has recently been confirmed by a x-ray photoelectron diffraction (XPD) study.[10] However, the size and distribution of metal islands including Ni on diamond surfaces have not yet been systematically investigated. One problem arises from charging effects which have hampered scanning tunnel microscope and scanning electron microscope studies on the morphology of the Ni-diamond interface.[11]

The growth of a flat monolayer or thin flat films of metals on semiconductor surfaces has not been possible for many systems[12] and only recently the formation of atomically flat Ag films at a critical thickness of 15 Å on a GaAs(110) surface has been observed.[13] This has been explained by a model that involves the stabilization of certain film thicknesses by quantized electrons of the adsorbed metal.[14,15] Thus, the electronic system of the adlayer governs the growth process as well as other factors like surface stress[16] and adatom kinetics.[17]

In the experiments reported here, high-resolution helium atom scattering (HAS) and x-ray photoelectron spectroscopy (XPS) have been used to study the initial stages of the growth of Ni on diamond H(1×1)C(111) at coverages less than 50 Å. The unique capabilities of the HAS technique, which can be equally well applied to metals, semiconductors, and insulators, to investigate structure and phonon-dynamics of diamond surfaces have been demonstrated in previous studies of clean H(1×1)C(111) surfaces in this laboratory.[18,19]

The paper is organized as follows. In the next section the

experimental setup and sample preparation are described. In the following section, HAS diffraction and XPS results are used to determine the growth mode, height distribution, and coverage of the Ni layers. *Inelastic* time-of-flight (TOF) HAS measurements are then presented in Sec. IV. These data allow to determine the phonon dynamics of the grown Ni islands. The paper concludes with a summary in Sec. V.

II. EXPERIMENTAL SETUP

The experiments were carried out in a helium atom scattering apparatus described in more detail elsewhere.[20] Briefly, the apparatus consists of a He atom beam nozzle source, a UHV target chamber, a time-of-flight tube and a homemade magnetic mass spectrometer for the detection of the He atoms. The target chamber is equipped with a back-view LEED, a Leybold-EA11 hemispherical electron energy analyzer, a Leybold double-anode x-ray source, and a homemade sample transfer system. The incident He atom beam has an energy spread $\Delta E/E_i$ of about 2%, which is independent of the incident energy E_i of the He atoms that can be varied between 12 and 80 meV corresponding to incident wave vectors $k_i = 4.8 - 12.4$ Å^{-1} by operating the source at temperatures between 40 and 400 K and at pressures between 40 and 700 bar.

Three different types of HAS measurements were carried out: (i) Angular distributions of He atoms scattered off the surface were recorded by rotating the crystal about an axis perpendicular to the plane formed by the incident and outgoing beams that have a fixed angle of 90.5°. The overall angular resolution of the apparatus amounts to 0.2°. (ii) The specular peak intensity was recorded as a function of incident wave vector by ramping the nozzle temperature from 40 to 400 K over a period of 1.5 h. These so-called ''drift-spectra'' are then plotted as intensity versus k_z curves, where k_z is the component of the scattering vector perpendicular to the surface. Maxima in these drift spectra correspond to constructive interference of outgoing waves. From the separation of those maxima the height of steps or islands on the surface can be deduced. (iii) Energy gains and losses of the He atoms due to inelastic scattering from surface phonons are detected over a wide range of angles using a time-of-flight (TOF) technique. These provide information on the surface phonon dispersion curves.

Three different (111)-oriented diamond type IIa samples[21] ($4 \times 4 \times 0.5$ mm^3) were used in the experiments. Two of them had miscuts of 2° and 4°, respectively. The third sample exhibited a misorientation of less than 0.25°. Differences in the experimental results obtained for these different diamond samples were not observed. Prior to the transfer into the UHV chamber the diamond surfaces were polished using a mixture of 1 μm Al_2O_3 powder and olive oil (20 min) and then pure olive oil (5 min) to saturate the surface with hydrogen. Finally, the sample was sonicated in acetone (15 min).[6] After the transfer into the UHV the surface was annealed to about 800 K for three hours in order to desorb all contaminants and residues from polishing. After this procedure the HAS-angular distributions closely resembled those recorded earlier for the H(1×1)C(111) surface.[18] XP spectra recorded after this annealing procedure did not reveal any contaminations (particularly oxygen) above the detection limit (5% of a monolayer). Ni was removed after each deposition by taking the substrate out of the UHV chamber and then applying the polishing and cleaning procedure described above.

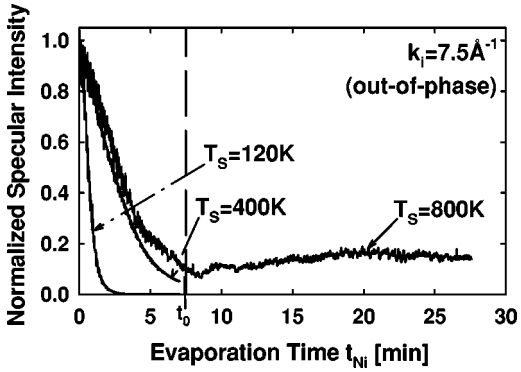

FIG. 1. The specular intensity is plotted versus evaporation time at three different substrate temperatures. $t_0 = 7.5$ min denotes a reference evaporation time.

Sample temperatures were independently measured by an alumel-chromel and a chromel-constantan thermocouple, respectively, both of which were attached to the static part (receiver) of the sample holder. Prior to the experiments the thermocouples were calibrated using a color pyrometer. Absolute temperatures given in this work are estimated to be accurate only within ± 50 K.

Nickel was evaporated from a Ni wire (diameter 0.5 mm, purity 99.995%) located about 5 cm away from the surface, which was heated resistively with currents of typically 5.5 A. After a thorough degassing procedure, the pressure during evaporation remained below 5×10^{-10} mbar. XP spectra recorded for the deposited Ni layers did not indicate the presence of any contaminations above the detection limit of the technique (5% of a monolayer).

III. GROWTH AND STRUCTURE OF Ni ON H(1×1)C(111)

A. Growth mode

Monitoring the He atom specular intensity during deposition is a convenient way to obtain information about the growth mode of a metal on a surface.[22] Three typical intensity vs. evaporation time, t_{Ni}, curves (''growth curves'') measured at different substrate temperatures, T_s, are shown in Fig. 1. All curves were recorded using the same Ni deposition rate. Initially the intensity decreases very rapidly with slopes that decrease for increasing T_s. The intensity then reaches a nearly constant value after about 2 and 8 min for $T_s = 120$ and $T_s = 800$ K, respectively. Oscillations in the specular intensity with deposition as seen in many other studies[23,24] were never observed even though both the deposition rate and surface temperatures were systematically varied. This observation excludes a layer-by-layer growth mechanism as observed for other metal-on-metal systems such as Pb/Cu(111) (Ref. 23) and Pt/Pt(111) (Ref. 24). Instead, the monotonic decay of the scattered intensity in Fig. 1 suggests that Ni does not form a *complete* first monolayer[25] on H(1×1)C(111). Such a monolayer would give rise to a (local) maximum in the reflectivity curves of Fig. 1, since the

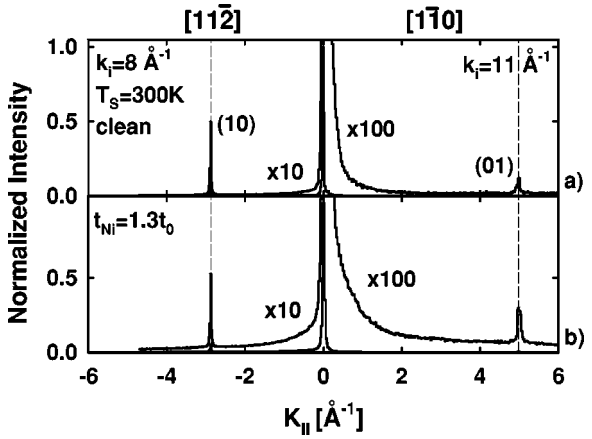

FIG. 2. (a) Angular distributions of the clean H(1×1)C(111) surface recorded along both the $[11\bar{2}]$ (left part) and the $[1\bar{1}0]$ (right part) azimuthal directions at $T_s=300$ K. The incident wave vectors are $k_i=8$ Å^{-1} and $k_i=11$ Å^{-1} for the $[11\bar{2}]$ and $[1\bar{1}0]$ azimuths, respectively. (b) The same as (a) for a Ni covered ($t_{Ni}=1.3t_0$) H(1×1)C(111) surface. The evaporation rate was the same as in Fig. 1. Ni was deposited at $T_s=800$ K.

concentration of defects, e.g., Ni adatoms, vacancies or steps, is generally expected to reach a local minimum upon completion of a monolayer. Thus it is concluded that Ni grows on H(1×1)C(111) by a 3D growth mode[26] for substrate temperatures up to $T_s=800$ K.

The factor of four difference in the initial slope of the He atom specular intensity curves for $T_s=800$ and $T_s=120$ K (Fig. 1) indicates an enhanced density of defects[27] in the films grown at lower substrate temperatures. This can be a consequence of either an increased adatom concentration on top of the Ni islands or an increased concentration of island boundaries possibly due to the formation of several *smaller* Ni islands at low temperatures. Most likely, however, both effects contribute to the low-residual intensities at lower temperatures and for this reason all the films were grown at $T_s=700-800$ K. The time at which the growth was stopped, t_{Ni}, is indicated in units of t_0 (see Fig. 1).

The question of whether Ni grows *epitaxially* on H(1×1)C(111) is addressed by comparing angular distributions recorded from the clean and Ni covered H(1×1)C(111) surface. Figures 2(a) and 2(b) display angular scans along both the $[1\bar{1}0]$ and $[11\bar{2}]$ azimuthal directions measured from a clean and a Ni covered ($t_{Ni}=1.3t_0$) H(1×1)C(111) surface. The angular scans of the clean surface [Fig. 2(a)] reveal sharp first-order diffraction peaks at the anticipated positions, which have already been discussed in earlier work.[18,19] Due to the different corrugation amplitudes along the $[1\bar{1}0]$ and $[11\bar{2}]$ azimuthal directions[28] the relative diffraction intensities along the $[1\bar{1}0]$ and the $[11\bar{2}]$ directions differ by approximately one order of magnitude. The first-order diffraction peaks of the Ni covered H(1×1)C(111) surface [Fig. 2(b)] are not shifted with respect to the peaks in Fig. 2(a) as can be clearly seen by the vertical dashed line. A splitting of the diffraction peaks or satellite peaks in the vicinity of the specular was not observed.

These findings reveal a true epitaxial growth mode of the Ni islands on the H(1×1)C(111) diamond substrate. Since the Ni-diamond lattice mismatch is only 1.4% the tensile stress within the islands is expected to be small. Closer inspection of Fig. 2 reveals an increased background and a broadening of the specular peak in the angular scan recorded from the Ni-covered H(1×1)C(111) surface.

The data presented so far are consistent with earlier results from LEED (Ref. 9) and XPD (Ref. 10) measurements, which report heteroepitaxial growth of Ni on H(1×1)C(111) up to substrate temperatures as high as 650°C. Deposition at room temperature was reported to lead to a poor ordering of the adsorbed layers in Ref. 9. Poor ordering corresponds to an enhanced concentration of defects in the Ni overlayer which is consistent with the steeper initial slopes at lower temperatures in the ''growth curves'' in Fig. 1 (see discussion above).

B. Island morphology and heights

The results reported so far reveal that Ni does not grow in a simple layer-by-layer mode but forms large three-dimensional (3D) islands already in the initial stage of adsorption. To gain information on the island heights, series of drift spectra (see Sec. II) were recorded for different Ni layers deposited at $T_s=800$ K with the same rate as for the measurements shown in Fig. 1 on the hydrogen terminated surface at $T_s=300$ K. The results and their interpretation are presented in Fig. 3. The gray curve in the upper panel has been recorded for a clean H(1×1)C(111) surface and agrees with previous measurements[19]. The difference Δk_z of subsequent maxima corresponds to a step height $h_{C(111)}=2\pi/\Delta k_z=2.1$ Å, which agrees well with the interlayer distance of diamond in the (111) direction. Sharp intensity maxima separated by about 0.3 Å^{-1} are observed in the drift spectrum (black solid line in the upper panel of Fig. 3) after Ni was deposited ($t_{Ni}=t_0$, cf. Sec. III A), indicating significant changes in the surface morphology. It is interesting to observe that the high-frequency oscillations for the Ni adlayer (black curve) is modulated by the drift spectrum seen for the clean substrate (gray curve). Hence, the drift spectrum of the Ni-covered surface shown in the upper panel can be unambiguously interpreted as a convolution of the substrate signal and that originating from the Ni islands. The period of the sharp oscillations corresponds to an island height of 20 Å.

For the incident He-atom energies used here the scattering process is mainly governed by the repulsive part of He-surface interaction potential.[29] Due to differences in the He-Ni(111) and He-H(1×1)C(111) interaction potentials the turning points of the He atoms are not expected to be located at the same distances above the diamond surface and the surface of the Ni islands, respectively. Consequently, the height h deduced from the simple relation $h=2\pi/\Delta k_z$ can not be regarded as the *true* height of the Ni islands. Previously published He atom-surface interaction potentials for He/H(1×1)C(111) (Ref. 30) and He/Ni(111) (Ref. 31) indicate, however, that the difference in the turning points is less than 0.2 Å. In the analysis presented below this small difference has been neglected.

The lower part of Fig. 3 shows enlarged sections from a series of drift spectra recorded at different Ni coverages with the same deposition rate as in Fig. 1. In order to more strongly emphasize differences in periodicity the interval be-

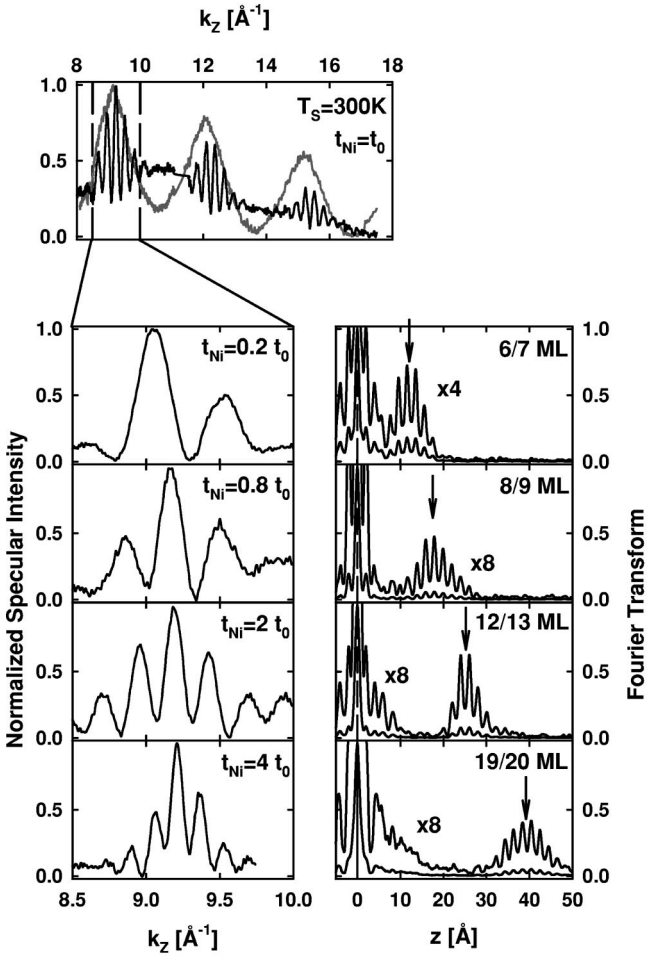

FIG. 3. Drift spectra recorded from the clean and Ni covered H(1×1)C(111) surfaces under specular conditions. The upper panel shows a spectrum recorded from the clean surface (gray curve), (see Sec. II) and a surface where Ni was evaporated for $t_{Ni}=t_0$ at $T_s=800$ K (black solid line). The panels below show a section (indicated by the vertical dashed lines in the upper panel) of drift spectra measured for H(1×1)C(111) where different amounts of Ni were deposited at $T_s=800$ K on an expanded k_z scale. Fourier transforms of the *whole* drift spectra are presented in the small panels on the right side. Vertical arrows indicate the position of the maxima of the island height distribution. The evaporation rate was the same as in Fig. 1.

tween $k_z=8.5$ and $k_z=10.0$ Å^{-1} is shown (indicated in the upper panel by vertical dashed lines) on an expanded scale. With increasing deposition time t_{Ni}, the separation between the maxima of the oscillations becomes smaller, indicating an increasing height of the Ni islands.

Assuming simple scattering kinematics the Fourier transformation of the diffraction pattern provides information on the distribution of island heights, as displayed in the right panels of Fig. 3. For this calculation the *full* k_z range of the drift spectra was taken into account. In addition to a peak at $z=0$ the Fourier transforms exhibit maxima spaced by about 2 Å corresponding to the step height of the diamond (111) substrate. For increasing deposition times the absolute maximum (denoted by an arrow) shifts from about 10 to 40 Å.

A simple, one-dimensional model was employed to interpret these results. As illustrated in Fig. 4(a), the diamond

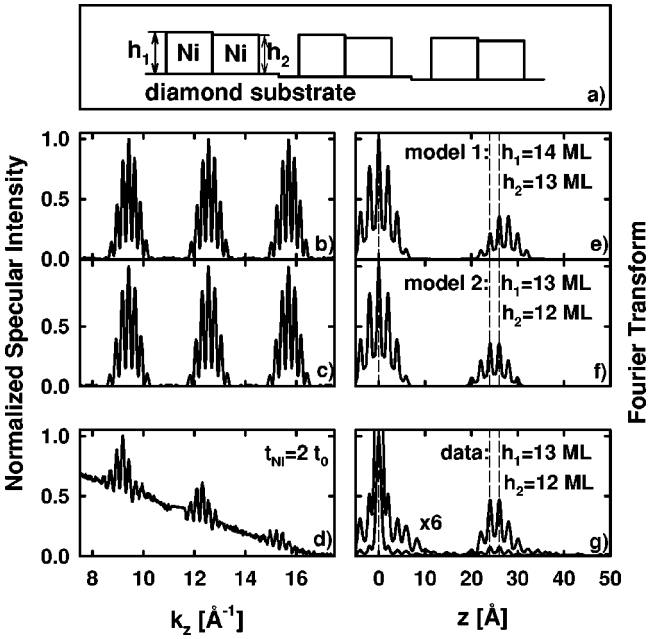

FIG. 4. (a) One-dimensional model of the Ni/H(1×1)C(111) interface. (b) Simulated drift spectrum for island heights $h_1=14$ ML, $h_2=13$ ML. (c) Same as (b), but for $h_1=13$ ML, $h_2=12$ ML. (d) Measured drift spectrum. The evaporation time was $t_{Ni}=2t_0$. The same deposition rate as in Fig. 1 was used. (e) Fourier transform of the simulated spectrum (b). (f) Same as (e), but for (c). (g) Fourier transform of the measured spectrum (d).

substrate was modeled by a periodic array of terraces separated by monoatomic steps with height $h_{C(111)}$. Ni islands of different heights, h_1 and h_2, were then placed on each terrace. Each island covers 25% of the terrace. The height of a monolayer has been set to the value of the separation of bulk Ni(111) planes, $h_{Ni(111)}=2.03$ Å. Using kinematic diffraction theory[32] the intensity in the specular direction ($K_{\|}=0$ Å^{-1}) can be calculated in a straightforward fashion. Results for two different examples with h_1 and h_2 corresponding to 13 and 14 monolayers (ML) and 12 and 13 ML are presented in Figs. 4(b) and 4(c), respectively. The simulated drift spectra in Figs. 4(b) and 4(c) agree well with the experimental data shown in Fig. 4(d).

Fourier transforms of the two simulated drift spectra in Figs. 4(b) and 4(c) are presented in Figs. 4(e) and 4(f). As expected the positions of the pronounced maxima [13/14 and 12/13 ML in Figs. 4(e) and 4(f), respectively] correspond to the heights of the Ni islands in the model. The other maxima correspond to interference of outgoing waves originating from different terraces. For example, constructive interference of waves scattered off an island with $h_1=14$ ML and an *adjacent* diamond terrace ($h_{Ni(111)}\approx h_{C(111)}$) gives rise to a peak at 15 ML in Fig. 4(e). The best agreement with the Fourier transform of the measured drift spectrum [Fig. 4(g)] has been achieved for the two-island model described above with island heights of 12 and 13 ML. This is illustrated by vertical dashed lines in Figs. 4(e)–4(g).

Similar calculations as described above were carried out for all drift spectra measured from the Ni/H(1×1)C(111) system at different Ni coverages. For each spectrum, the best agreement was achieved with a model using two island heights only. Our results are summarized in Table I. The

TABLE I. Determination of the heights of the Ni islands in monolayers (ML) from the measured heights h_1 and h_2 and the bulk separation $h_{Ni(111)}$, see text. Ni was deposited at $T_s = 800$ K. The deposition time, t_{Ni}, is expressed in units of the reference time, t_0 (Fig. 1). ML(1) and ML(2) are the estimated thicknesses in monolayers of islands with heights h_1 and h_2, respectively.

t_{Ni}/t_0	h_1 [Å]	h_2 [Å]	$h_1/h_{Ni(111)}$	$h_2/h_{Ni(111)}$	ML(1)	ML(2)
0.2	13.6	11.6	6.7	5.7	7	6
0.8	17.9	15.9	8.8	7.8	9	8
1	22.05	20.0	10.9	9.9	11	10
2	26.0	24.0	12.8	11.8	13	12
4	40.4	38.4	19.9	18.9	20	19

integer values given in the last two columns are considered to be the true heights (in monolayers) of the Ni islands.

Although an overall layer-by-layer growth of Ni on the H(1×1)C(111) surface (Fig. 1) was not found the growth mechanism of the islands is not completely 3D. On the contrary, our data suggest that the island height distribution is very narrow. The majority of the Ni islands on the surface has heights of either n or $n+1$ monolayers, where n is a function of the deposited amount of Ni alone. Therefore we conclude, that the *local* (i.e., for a particular island) growth mode is actually a layer-by-layer mode.

The specular peak in the angular distributions recorded from the Ni-covered surface is considerably broadened compared to the clean surface (cf. Fig. 2). If a simple geometric distribution of the Ni islands is assumed the profile of the specular beam can be described by a formula that includes the average width of the islands as a fit parameter.[33] Such an analysis was carried out for a surface covered by Ni islands with heights of 10/11 ML. The best fit yields an average diameter of the Ni islands of 55 Å.

Our data also provide an important piece of information on the very onset of the island growth: (i) additional oscillations in drift spectra for deposition times, t_{Ni}, less than $0.2t_0$ (or the equivalent if the deposition rate was different) were never observed, and (ii) island heights less than 6 ML were never found. This favors a scenario where the growth starts with small, 6 ML-thick islands even for very small coverages. However, lateral size and concentration of the islands have to exceed a certain minimum value to contribute considerably to the coherent diffraction pattern (drift spectrum). As shown below, a deposition time $t_{Ni} = 0.2t_0$ corresponds indeed to a situation where almost 50% of the diamond surface is already covered by Ni islands.

C. Coverage

The Ni-island coverage was determined by recording XP spectra simultaneously with the He atom scattering data. Prior to the experiments presented here reference XP spectra from the clean H(1×1)C(111) surface (C 1s peak at 284 eV) and a polycrystalline Ni sample (Ni $2p_{1/2}$ at 870 eV and $2p_{3/2}$ at 852 eV) were recorded. In terms of a simple model[34] the attenuation of the C 1s signal due to the presence of Ni islands for normal emission can be written as

$$I_C/I_C^0 = \Theta \exp(-h/\lambda_C) + (1-\Theta), \quad (1)$$

where I_C is the measured intensity of the C 1s peak after background subtraction, I_C^0 is the intensity measured from the clean diamond substrate, Θ is the amount of the H(1×1)C(111) surface covered with Ni and λ_C is the mean free path of the emitted C 1s photoelectrons in Ni [$\lambda_C = 13.6$ Å (Ref. 34)]. To keep the model simple an average island height h, $h = (h_1 + h_2)/2$ is used. A different expression describes the increase of the Ni 2p intensity for normal emission,

$$I_{Ni}/I_{Ni}^0 = \Theta(1 - \exp[-h/\lambda_{Ni}]). \quad (2)$$

I_{Ni} and I_{Ni}^0 are the Ni 2p intensities (sum of the Ni $2p_{1/2}$ and Ni $2p_{3/2}$ peaks) measured from the Ni-covered diamond surface and the Ni sample described above, respectively. The mean free path of the Ni 2p photoelectrons amounts to $\lambda_{Ni} = 7.5$ Å.[34] Equations (1) and (2) allow the simultaneous determination of the properties Θ and h. Since the height h was determined very precisely from the drift spectra (see above) both Eq. (1) and Eq. (2) were used to determine the coverage Θ. The results, summarized in Table II, provide a rough measure (estimated error: ±15%) for the Ni-covered area of the diamond surface, although the agreement between the coverages calculated from Eq. (1) and Eq. (2) is not completely satisfactory. For further discussion an average coverage Θ_{Ni} (last column in Table II) was calculated. Even at the lowest island heights (6/7 ML) about 50% of the H(1×1)C(111) surface is covered by Ni islands.

IV. PHONON DYNAMICS OF Ni ISLANDS ON H(1×1)C(111)

A. TOF measurements

Figures 5(a) and 5(b) show two series of TOF spectra converted to an energy transfer scale recorded for a diamond H(1×1)/C(111) surface covered by 10.5 ML of Ni along

TABLE II. Results of the determination of the coverage Θ for different island heights using independently the C 1s [Eq. (1)] and the Ni 2p [Eq. (2)] XPS signals. Θ_{Ni} is the average coverage calculated from columns two and three.

ML	Θ from C 1s	Θ from Ni 2p	Θ_{Ni}
6/7	0.51	0.42	0.47
8/9	0.65	0.55	0.60
10/11	0.61	0.59	0.60
12/13	0.76	0.68	0.72
19/20	0.80	0.95	0.88

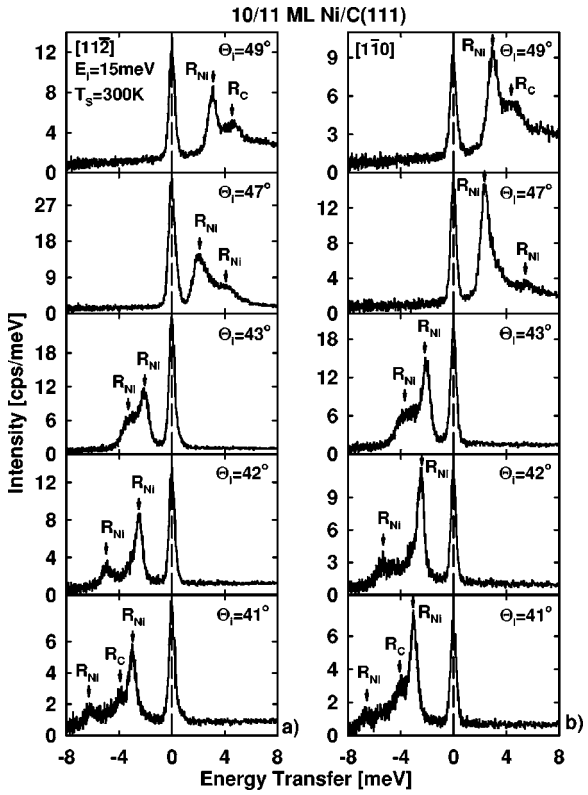

FIG. 5. Series of TOF spectra recorded from Ni islands of a heights 10/11 ML on the H(1×1)C(111) surface. (a) [11$\bar{2}$]-azimuth. (b) [1$\bar{1}$0]-azimuth.

the [11$\bar{2}$] and [1$\bar{1}$0] azimuthal direction. Inelastic peaks (denoted by R_{Ni}) originating from the adsorbed Ni islands (10/11 ML) can be identified by comparison to corresponding data for the clean H(1×1)C(111) surface.[18] The full width half maximum (FWHM) and the relative intensities of the R_{Ni} peaks are similar to the inelastic features observed in the HAS-TOF spectra of close packed clean metal surfaces.[35] This observation indicates a high structural quality of the adsorbed Ni islands, in agreement with the results of the structural analysis, see Sec. III. The Rayleigh mode of the H(1×1)C(111) surface[18] is also seen in these spectra and is denoted by R_C in Fig. 5. The experimental observation of the R_C mode indicates that under the conditions given in Fig. 5 the surface is not completely wet by the Ni film. This is consistent with the results in Table II.

The measured data are collected in the dispersion plot presented in Fig. 6(a). Scan curves (solid lines) including those corresponding to the TOF spectra of Fig. 5(b) are also shown to illustrate how each particular TOF energy loss peak contributes to the phonon dispersion curves in the vicinity of the $\bar{\Gamma}$ point. Neither for annihilation ($\Delta E>0$) nor for creation ($\Delta E<0$) do the points pass through the origin of the plot as it is customary for well-defined single crystal surfaces. Rather they reveal a zone center gap of $E_{gap}=2.15$ meV. The open circles indicate the location of the Rayleigh mode of the substrate R_C. The phonon dispersion curves along both azimuthal directions have been measured for several island heights. Three typical curves are shown together with earlier published electron-energy loss spectra (EELS) data[36] recorded for a Ni(111) surface along the [11$\bar{2}$] direction in Fig. 6(b). With increasing Ni island height the gap energy decreases to $E_{gap}=1$ meV for 20 ML Ni as indicated by the horizontal arrows in Fig. 6(b).

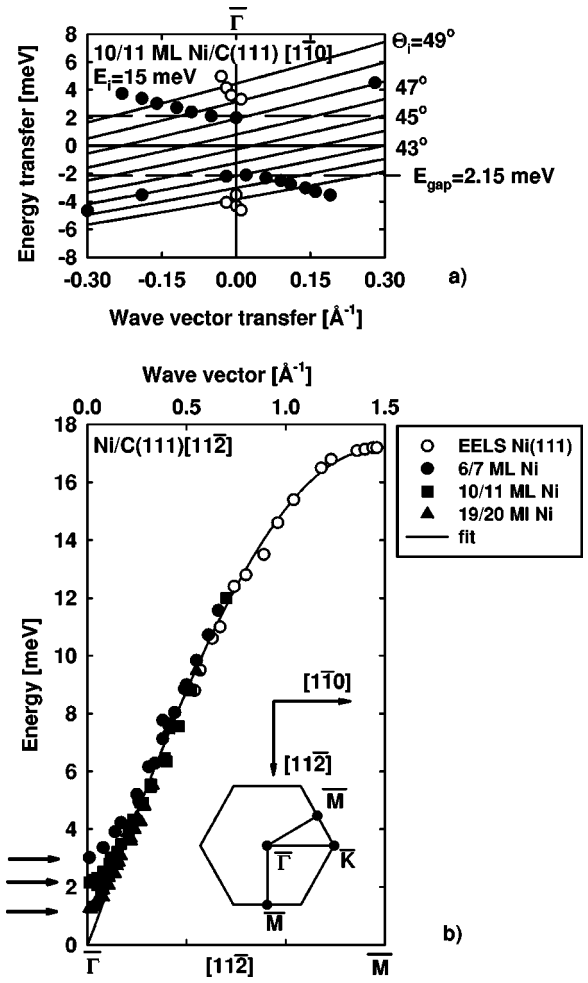

FIG. 6. (a) Dispersion plot corresponding to the TOF spectra of Fig. 5(b). The filled circles represent the inelastic events corresponding to the mode R_{Ni} in Fig. 5(b) whereas the open circles show the Rayleigh mode R_C of the H(1×1)C(111) substrate. Additionally, the scan curves (see text) corresponding to the incident angles Θ_i in Fig. 5(b) are shown. (b) Experimentally determined surface phonon dispersion curves for Ni islands on H(1×1)C(111) with heights of 6, 10, and 21 ML along the [11$\bar{2}$] direction. The horizontal arrows denote the different zone center gaps. The Rayleigh mode R_C of the substrate is not shown. The open circles show EELS data recorded from Ni(111) of Menezes *et al.* (Ref. 36), the solid line represents the best fit of those data using a slab calculation based on a single-force constant model.

The measured values of the gap energy E_{gap} are summarized in Fig. 7(a). E_{gap} is a monotonous function of the Ni island height, a given height h corresponds to a well-defined (see TOF spectra Fig. 5) energy E_{gap}.

B. Lattice dynamic analysis

The vibration gap at the $\bar{\Gamma}$ point corresponds to a periodic displacement of the Ni islands normal to the substrate surface. The presence of a similar zone center gap has also been observed for thin alkali metal films on Cu(001).[37] In this case the so-called organ pipe modes localized within the alkali

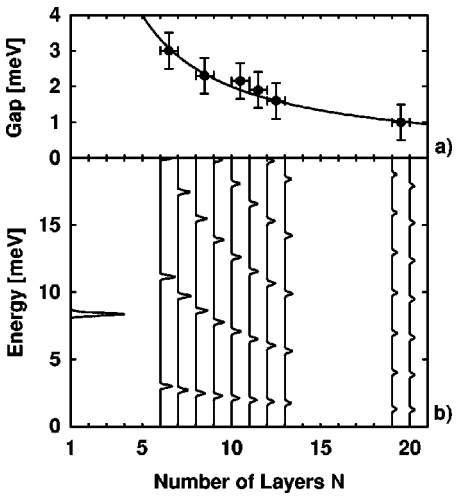

FIG. 7. (a) Measured zone center gap energies plotted versus the number of layers in the Ni islands (filled circles). Since each data point corresponds to two island heights (see text), n and $n+1$ layers, the symbols are placed at $n+\frac{1}{2}$ layers. This uncertainty is indicated by a horizontal error bar. The solid line shows a least square fit to the data. (b) Calculated densities of states of the z-polarized modes at the surface Ni atom for 1, 6-13, 19, and 20 ML Ni on a rigid substrate at the $\bar{\Gamma}$-point. The resulting DOS was convoluted with a Gaussian function with a FWHM of 0.25 meV.

metal layers are nearly dispersionless and the experimental TOF spectra reveal several overtone excitations. According to Ref. 38 the strength of the adsorbate-substrate coupling can be described by a parameter γ, which is obtained from a fit of the variation of E_{gap} with the number N of adsorbed layers

$$E_{gap}=E_1 N^{-\gamma}, \tag{3}$$

were E_1 is the extrapolated gap energy of a 1 ML film. A least square fit of the data in Fig. 7(a) shown by the continuous line curve yields $\gamma\approx 0.95$ and $E_{gap}=11$ meV. The fitting procedure is hampered by the fact that data for Ni island heights less than 6 ML are not available. The value for γ is close to the upper limit of $\gamma=1$ discussed in Ref. 38 and indicates a strong substrate-adsorbate interaction. Since, however, in our case the Ni-atoms are expected to be only weakly adsorbed on the H-terminated surface the present result indicates that this simple model is not applicable to the system studied here.

A full lattice dynamics analysis was carried out to gain more insight into the phonon dynamics of the system and to confirm our interpretation of the observed vibrations at the $\bar{\Gamma}$ point. For the calculations a rigid substrate model has been used, which is well justified because of the large mismatch in force constants between substrate and adsorbate. The substrate-Ni force constant $\bar{f}^R_{CNi}$ was obtained from a fit to the measured value $E_{gap}=3$ meV for islands with a height $h=6/7$ ML, the result is $\bar{f}^R_{CNi}=15.75$ N/m. The lattice dynamics of Ni can be described by one nearest-neighbor radial force constant f^R_{NiNi} (similar to copper[39]) a least square fit to the only data available for the Ni(111) surface[36] yields $f^R_{NiNi}=43$ N/m. The result of this fit of the Rayleigh phonon of the Ni(111) surface is shown in Fig. 6(b) (solid line). For comparison with the force constant $\bar{f}^R_{CNi}$, f^R_{NiNi} is converted to an interlayer force constant $\bar{f}^R_{NiNi}$ between Ni(111) planes,[38] $\bar{f}^R_{NiNi}=86$ N/m. The ratio $\bar{f}^R_{CNi}/\bar{f}^R_{NiNi}=0.18$ indicates a coupling between the adsorbate (Ni) and the substrate, which is weak compared to the Ni-Ni interaction. This is in contrast to the result for the parameter γ [Eq. (3)] and suggests that the character of the adsorbate-substrate interaction cannot be determined from Eq. (3) alone. Densities of states (DOS) of the z-polarized vibrations projected on the Ni *surface* layer were calculated for several numbers of Ni layers using the rigid substrate model. The results are plotted in Fig. 7(b). The lowest calculated energies agree well with the measured values for each Ni island height. The calculated DOS for 1 ML Ni has a strong peak at 8 meV which corresponds to the vibration energy of 1 ML Ni on H(1×1)C(111). This energy agrees roughly with the value $E_1=11$ meV obtained from the simple model discussed above [Eq. (3)]. Figure 7(b) also shows additional modes (overtones) at higher vibration energies for layer numbers $N>1$. Contrary to the case of alkali metal overlayers[37] overtone modes were never observed in the experimental TOF spectra recorded from Ni covered H(1×1)C(111) surfaces (cf. Fig. 5). The absence of overtones is not surprising since the Ni/H(1×1)C(111) system ($\bar{f}^R_{CNi}/\bar{f}^R_{NiNi}=0.18$) does not fulfill the condition for the appearance of open standing waves (organ-pipe condition, $f_{sa}/f_{aa}=2$, f_{sa} and f_{aa} are the substrate-adsorbate and the adsorbate-adsorbate force constants, respectively[38]).

The width of the R_{Ni} peaks in the TOF spectra is small and comparable to the FWHM of the substrate phonon peaks (R_C). This indicates that not only the coupling of the adlayer phonons to the stiff substrate is small as expected, but also independently demonstrates that the island height distribution is very narrow. Figure 7(a) as well as our calculations show a strong correlation of the vibration energy and island height. The presence of Ni islands with different heights (i.e., a variation in height of several monolayers from island to island) would lead to a broadening of the R_{Ni} peaks in the TOF spectra due to the superposition of phonon peaks originating from islands with different heights and corresponding different phonons frequencies. The width of the R_{Ni} peaks in Fig. 5, however, corresponds to the experimental resolution. Thus, the phonon dynamics of the Ni/H(1×1)C(111) system is fully consistent with the picture of the growth mode of Ni on H(1×1)C(111) as given in Sec. III.

V. SUMMARY AND CONCLUSIONS

The adsorption of Ni onto the H(1×1)C(111) diamond surface has been studied by high resolution helium atom scattering and x-ray photoelectron spectroscopy (XPS). The experimental results presented here provide the first complete set of structural and dynamical data of metal adlayers on a diamond substrate. Upon deposition at $T_s=800$ K, Ni forms large islands with heights ranging from 6 to 20 ML and diameters of about 50 Å. The height distribution of the islands on the well defined, atomically flat diamond surface is very narrow as schematically depicted in Fig. 8. The islands are found to cover between 50 and 85 % of the surface. A single island grows epitaxially in a layer-by-layer fashion,

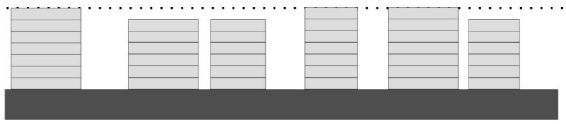

FIG. 8. Schematic drawing showing the morphology of Ni islands grown epitaxially on the H(1×1)/C(111) diamond substrate for deposition at 800 K. Noteworthy is the large diameter of the Ni islands (>55 Å) and the very uniform height distribution.

more detailed studies on this apparently new growth mode are presently under way. Deposition at room temperature is found to result in the formation of poorly ordered adlayers, which most likely consist of many small Ni islands with a much broader height distribution, in agreement with previous studies.[9]

The formation of atomically flat islands of transition metals on insulator surfaces was reported earlier.[3] Using transmission electron microscopy the formation of flat Pd islands on MgO(001) has been observed.[40] A combined spot profile analysis LEED and XPS study[41] on the deposition of Ni on the basal plane of graphite shows a temperature-dependent growth mode. At low temperatures (T_s=90 K), Ni forms (111) islands with uniform height, which is independent of the Ni coverage, while deposition at room temperature results in the formation of large clusters. These findings are in contrast to the data presented here for Ni/H(1×1)C(111), where a uniform but coverage dependent Ni-island height was found for *high* deposition temperatures.

Since metals do not wet insulator substrates, generally a 3D growth mode is expected. At low temperatures, however, the formation of 3D islands can be kinetically hindered since the metal atoms may not be able to overcome the activation barrier for hopping from the substrate to the top of the metal island.[3] As a consequence, the metal grows in a so-called pseudo-layer-by-layer growth mode[3] as was demonstrated for the adsorption of Cu on the $ZnO(000\overline{1})$ surface.[5] At T_s =130 K, Cu forms 2D (i.e., one atom layer thick) islands on the ZnO substrate until a coverage of 55% is reached.

For Ni/H(1×1)C(111), a somewhat different growth mode was observed at relatively high temperatures, T_s =800 K. Ni initially forms islands with heights of 6 to 7 ML before it starts to grow in a layer-by-layer mode. The reason for the existence of this minimum in thickness (6 ML) is presently not known. It seems unlikely that the growth process is kinetically hindered at temperatures as high as T_s =800 K. In fact, for the Cu/ZnO system mentioned above the formation of 3D Cu clusters is reported at T_s=800 K.[5] If the observed minimum thickness of 6 ML presents another instance of a metal film with a so-called ''magic'' thickness as suggested in Ref. 13 cannot be decided on the basis of our data and requires further investigations.

Since Ni is not a free electron metal the ''electronic growth'' model[14] cannot be used directly to explain the existence of ''magic'' thicknesses in the system Ni/H(1×1)C(111). We speculate however, that also in this case Ni-layers for thicknesses of less than 6 layers are unstable with regard to the formation of 3D clusters, as suggested in the work by Gavioli *et al.*[15] for the case of Ag.

The presence of large (>55 Å), structurally well-defined islands with a very narrow height distribution on the diamond substrate opens the unique possibility to investigate properties of 2D metals adlayers. Here, the phonon dispersion curves of the layers could be studied as a function of thickness. For the transverse acoustic mode polarized normal to the substrate a gap is observed at the $\overline{\Gamma}$ point, which decreases from 3 meV for the smallest thickness investigated (6 ML) to 1 meV for 20 ML. The lattice dynamical analysis of this gap energy reveals a weak coupling between the substrate and the Ni overlayer, indicating the absence of chemical interactions. The Rayleigh modes of the Ni islands and the Ni(111) surface can be described by the same radial force constant f^R_{NiNi}. This result suggests that the electronic properties of the Ni islands and (bulk) Ni(111) are identical, even for island heights as low as 6 ML. As a result of the large electronic band gap of diamond also electronic systems of the surface and the adlayer should be largely decoupled, the Ni islands on H(1×1)C(111) can thus be regarded as a model system for thin, virtually free-standing metal films. Therefore, the present Ni/H(1×1)C(111) should be of interest in connection with further experiments, which will comprise the investigation of chemical (adsorption of molecules, oxidation) and electronic properties of the islands as function of the island-height.

ACKNOWLEDGMENTS

We thank Dr. G. Witte (Bochum) for discussions and for comments on the manuscript. We also thank Dr. Th. Schaich (Heidelberg) for help in the initial stages of the experiment.

[1] H. Brune, Surf. Sci. Rep. **31**, 121 (1998); J.A. Venables, Surf. Sci. **299/300**, 798 (1994); C. Argile and G.E. Rhead, Surf. Sci. Rep. **10**, 277 (1989).
[2] E.W. Plummer and P.A. Dowben, Prog. Surf. Sci. **42**, 201 (1993).
[3] C.T. Campbell, Surf. Sci. Rep. **27**, 1 (1997).
[4] A. Zangwill, *Physics at Surfaces* (Cambridge University Press, Cambridge, 1988), p. 428.
[5] K.-H. Ernst, A. Ludviksson, R. Zhang, J. Yoshihara, and C.T. Campbell, Phys. Rev. B **47**, 13 782 (1993).
[6] B.B. Pate, Surf. Sci. **165**, 83 (1986).
[7] H. Kawarada, Surf. Sci. Rep. **26**, 205 (1996).
[8] K. Das, V. Venkatesan, K. Miyata, D.L. Dreifus, and J.T. Glass, Thin Solid Films **212**, 19 (1992).
[9] P.G. Lurie and J.M. Wilson, Surf. Sci. **65**, 453 (1977).
[10] O.M. Kuettel, J. Osterwalder, L. Schlapbach, and R. Agostino, Diamond Relat. Mater. **2**, 548 (1993).
[11] J. van der Weide and R.J. Nemanich, Phys. Rev. B **49**, 13 629 (1994).
[12] V.A. Grazhulis, Prog. Surf. Sci. **36**, 89 (1991); W.G. Schmidt, F. Bechstedt, and G.P. Srivastava, Surf. Sci. Rep. **25**, 141 (1996).
[13] A.R. Smith, K.-J. Chao, Q. Niu, and C.-K. Shih, Science **273**, 226 (1996).
[14] Z.Y. Zhang, Q. Niu, and C.-K. Shih, Phys. Rev. Lett. **80**, 5381 (1998).

[15] L. Gavioli, K.R. Kimberlin, M.C. Tringides, J.F. Wendelken, and Z. Zhang, Phys. Rev. Lett. **82**, 129 (1999).
[16] R. Koch, J. Phys.: Condens. Matter **6**, 9519 (1994).
[17] Z.Y. Zhang and M.G. Lagally, Science **276**, 377 (1997).
[18] G. Lange and J.P. Toennies, Phys. Rev. B **53**, 9614 (1996).
[19] Th. Schaich, J. Braun, J.P. Toennies, M. Buck, and Ch. Wöll, Surf. Sci. **385**, L958 (1997).
[20] B.J. Hinch, A. Lock, H.H. Madden, J.P. Toennies, and G. Witte, Phys. Rev. B **42**, 1547 (1990).
[21] The samples were provided by Drukker International BV, Beversestraat 20, 5431 SH Cuijk, The Netherlands.
[22] A. Sánchez, J. Ibañez, R. Miranda, and S. Ferrer, Surf. Sci. **178**, 917 (l986).
[23] B.J. Hinch, C. Koziol, J.P. Toennies, and G. Zhang, Europhys. Lett. **10**, 341 (1989).
[24] R. Kunkel, B. Poelsema, L.K. Verheij, and G. Comsa, Phys. Rev. Lett. **65**, 733 (1990).
[25] The term complete monolayer refers to an area with a typical diameter equal to the transfer width of the apparatus (about 150 Å) on the surface that is covered with a monatomic layer.
[26] E. Bauer, Appl. Surf. Sci. **11/12**, 479 (1982).
[27] B. Poelsema and G. Comsa, *Scattering of Thermal Energy Atoms from Disordered Surfaces* (Springer, Berlin, 1989).
[28] G. Lange, Ph.D. thesis, Göttingen, 1996.
[29] N. Esbjerg and J.K. Norskov, Phys. Rev. Lett. **45**, 807 (1980).
[30] G. Vidali, M.W. Cole, and W.H. Weinberg, Phys. Rev. Lett. **51**, 118 (1983).
[31] K. Lenarcic-Poljanec, M. Hodoscek, D. Lovric, and B. Gumhalter, Surf. Sci. **251/252**, 706 (1991).
[32] M. Henzler, in *Electron Spectroscopy for Surface Analysis*, edited by H. Ibach (Springer, Berlin, 1977), p. 117.
[33] C.S. Lent and P.I. Cohen, Surf. Sci. **139**, 121 (1984).
[34] G. Ertl and J. Küppers, *Low Energy Electrons and Surface Chemistry* (VCH, Weinheim, 1985).
[35] U. Harten, J.P. Toennies, and Ch. Wöll, Faraday Discuss. Chem. Soc. **80**, 137 (1985); U. Harten, J.P. Toennies, Ch. Wöll, and G. Zhang, Phys. Rev. Lett. **55**, 2308 (1955); G. Witte, J.P. Toennis, and Ch. Wöll, Surf. Sci. **323**, 228 (1995); J. Braun, K.L. Kostov, G. Witte, L. Surnev, J.G. Skofronick, S.A. Safron, and Ch. Wöll, *ibid.* **372**, 132 (1997).
[36] W. Menezes, P. Knipp, G. Tisdale, and S.J. Sibener, Phys. Rev. B **41**, 5648 (1990).
[37] G. Benedek, J. Ellis, A. Reichmuth, P. Ruggerone, H. Schief, and J.P. Toennies, Phys. Rev. Lett. **69**, 2951 (1992).
[38] N.S. Luo, P. Ruggerone, and J.P. Toennies, Phys. Rev. B **54**, 5051 (1996).
[39] J. Ellis, J.P. Toennies, and G. Witte, J. Chem. Phys. **102**, 5059 (1995).
[40] C.R. Henry, C. Chapon, C. Duriez, and S. Giorgio, Surf. Sci. **253**, 177 (1991).
[41] M. Bäumer, J. Libuda, and H.-J. Freund, Surf. Sci. **327**, 321 (1995).